Relative efficiency of a chain sweep and the rockhopper sweep used for the NEFSC bottom trawl survey and chainsweep-based swept area biomass estimates for 11 flatfish stocks

Timothy J. Miller[1], Phil Politis[1], Jessica Blaylock[1], David Richardson[2], John Manderson[3], and Chris Roebuck[4]

[1]Northeast Fisheries Science Center, 166 Water Street, Woods Hole, MA 02543 USA
[2]Northeast Fisheries Science Center, Naragansett, RI USA
[3]Northeast Fisheries Science Center, National Marine Fisheries Service, Sandy Hook, NJ USA
[4]F/V Karen Elizabeth, Pt. Judith, RI, USA

Abstract

Using a general hierarchical model we estimated relative efficiency of chain sweep to the rockhopper sweep used by the NEFSC bottom trawl survey for six species of flatfish (summer flounder, American plaice, windowpane, winter flounder and yellowtail flounder) from three studies carried out in 2015-2017 aboard the F/V Karen Elizabeth twin trawl vessel. Aside from the sweeps, the rest of the trawl gear is the same. We compared a set of models with different assumptions about variation of relative efficiency between paired gear tows, size and diel effects on the relative efficiency, and extra-binomial variation of observations within paired gear tows. The best models for each species included size effects on and variation in relative catch efficiency between each observation. Diel effects provided improved model performance for summer flounder, windowpane, winter flounder, and witch flounder. We used the best performing models with and without model parameters that differ for tows conducted during day and night to make and compare annual chain sweep-based swept area biomass estimates for 11 stocks during the spring and fall surveys under the alternative assumptions. We estimated uncertainty in all results using bootstrap procedures for each data component.

Introduction

Paired-gear studies have long been used to estimate the efficiency of one fishing gear relative to another (e.g., Gulland 1964; Bourne 1965). These types of studies are critical for informing abundance time series from fishery independent surveys when there are changes in the vessel and(or) gears over time due to gear failures or improved technology.

In conducting paired-gear studies it is ideal to have the two gears deployed as close together spatailly and temporally as possible to reduce variation between the gears in densities of the species being captured. One fishing method that approaches this ideal is the twin-trawl rigging where two trawls can be fished simultaneously (ICES 1996).

Here we expand the methods of Miller (2013) to also evaluate diel effects on relative catch efficiency and estimate for 6 flatfish species: American plaice (*Hippoglossoides platessoides*), summer flounder (*Paralichthys dentatus*), windowpane (*Scophthalmus aquosus*), winter flounder (*Pseudopleuronectes americanus*), witch flounder (*Glyptocephalus cynoglossus*), and yellowtail flounder (*Limanda ferruginea*). We also use the relative catch efficiency estimates to estimate chain-sweep swept area biomass for 11 stocks (2 for windowpane, and 3 each for winter flounder and yellowtail flounder) in the Northeast fisheries Science Center spring and fall bottom trawl surveys.

Methods

Data collection

Data were collected during three field experiments carried out in 2015, 2016, and 2017, respectively, aboard the F/V Karen Elizabeth, a 78ft stern trawler capable of towing two trawls simultaneously side by side. One side of the twin-trawl rig towed a NEFSC standard 400 x 12 cm survey bottom trawl rigged with the NEFSC standard rockhopper sweep (Politis et al. 2014) (Figure 1). The other side of the twin-trawl rig towed a version the NEFSC 400 x 12cm survey bottom trawl modified to maximize the capture of flatfish. The trawl was modified by reducing the headline floatation from 66 to 32, 20cm, spherical floats, reducing the port and starboard top wing-end extensions by 50cm each and utilizing a chain sweep. The chain sweep was constructed of 1.6cm (5/8in) trawl chain covered by 12.7cm diameter x 1cm thick rubber discs on every other chain link (Figure 2). Two rows of 1.3cm (1/2in) tickler chains were attached to the 1.6cm trawl chain by 1.3cm shackles (Figure 2). To ensure equivalent net geometry of each gear, 32m restrictor ropes, made of 1.4cm (9/16in) buoyant, Polytron rope, were attached between each of the trawl doors and the center clump. 3.4m2 Thyboron Type 4 trawl doors were used to provide enough spreading force to ensure the restrictor ropes remained taut throughout each tow. Each trawl used the NEFSC standard 36.6m bridles. All tows followed the NEFSC standard survey towing protocols of 20 minutes at 3.0 knots. In 2015, 108 (45 day, 63 night) paired tows were conducted in eastern Georges Bank and off of southern New England (Figure 3). In 2016, 117 (74 day, 43 night) paired tows were conducted in western Gulf of Maine and northern edge of Georges Bank (Figure 4). In 2017, 103 (61 day, 42 night) paired tows were conducted in waters off of southern New England (Figure 5). The number of paired tows where a given species was captured ranged betweeen 132 and 186 (Table 1).

Paired-tow analyses

We use the hierarchical modeling approach from Miller (2013) to estimate the relative efficiency of chain sweep to the rockhopper sweep used by the NEFSC bottom trawl survey for six species from three studies carried out aboard a twin trawl vessel. Aside from the sweeps the rest of the trawl gear is the same. As in Miller (2013), we compared a set of models with different assumptions about variation of relative efficiency between paired gear tows, size effects on the relative efficiency, and extra-binomial variation of observations within paired gear tows. However, we further expand the models to investigate diel effects on the relative efficiency. The analyses are analogous to those by Miller et al. (2017a,b), but updated to include data collected in 2017. We estimate biomass for 11 stocks in the annual fall and spring surveys between 2009 and 2016 assuming the chain sweep is fully efficient. The best performing models with and without model parameters that differ for tows conducted during day and night are used to make and compare biomass estimates under the alternative assumptions. We estimated uncertainty in all results using bootstrap procedures for each data component.

Like the analyses in Miller et al. (2017a,b), we fit the same set of 13 models described in Miller (2013), and reproduced here in Tables 2 and 3, to all data combined and also to data for observations conducted during the day and night, separately. The latter set of fits together equate to a model with all parameters differing by whether the tows were conducted duing the day or night. Day and night tows were defined by whether the sun was above the horizon at the time of the tow.

For all the models fitted to the twin trawl data, the length-weight data, and the survey data, parameter estimation was performed by maximizing the model likelihood programmed in TMB (Kristensen et al. 2016) and R (R Core Team 2017).

Length-weight analysis

We used the length and weight observations for each survey to estimate a survey-specific length-weight relationship. We assumed weight observation j from survey i, was log-normal distributed,

$$\log W_{ij} \sim \mathrm{N}\left(\log \alpha_i + \beta_i \log L_{ij} - \frac{\sigma_i^2}{2}, \sigma_i^2\right) \tag{1}$$

We used a bias correction to ensure the expected weigth $E(W_{ij}) = \alpha_i L_{ij}^{\beta_i}$.

Biomass estimation

We estimated biomass for each annual survey using two approaches. The first does not account for any diel effects on the relative efficiency of the rockhopper sweep to chain sweep gear whereas the second approach does account for diel differences in the relative efficiency. In some tows for the NEFSC surveys there may be subsampling when a large number of a given species are caught, but we used the extrapolated numbers at length for such tows. For the first approach

$$\widetilde{N}_{1hi}(L) = N_{hi}(L)\,\widehat{\rho}(L) \tag{2}$$

where $N_{hi}(L)$ is the number at length L in tow i from stratum h and $\widehat{\rho}(L)$ is the relative efficiency of the chain sweep to rockhopper sweep at length L estimated from the twin trawl observations in a model without diel effects on the relative efficiency. Note that we have omitted any subscripts denoting the year or survey. For the second approach

$$\widetilde{N}_{2hi}(L) = N_{hi}(L)\,\widehat{\rho}(L,D)^{I_{hi}(D)}\,\widehat{\rho}(L,N)^{1-I_{hi}(D)} \tag{3}$$

where $\widehat{\rho}(L,D)^{I_{hi}(D)}$ and $\widehat{\rho}(L,N)$ are the relative efficiency of the chain sweep to rockhopper sweep at length for daytime and nighttime tows, respectively, estimated from the twin trawl observations in a model with diel effects on the relative efficiency, and $I_{hi}(D)$ is the indicator variable of whether tow i was conducted during the daytime.

The stratified abundance estimate is then calculated using the design-based estimator,

$$\widehat{N}_g(L) = \sum_{h=1}^{H} \frac{A_h}{An_h} \sum_{i=1}^{n_h} \widetilde{N}_{g,h,i}(L) \tag{4}$$

where g indicates which abundance at length per tow is used (eq. 2 or 3), A_h is the area of stratum h, $A = \sum_{h=1}^{H} A_h$, and n_h is the number of tows that were made in stratum h. The corresponding biomass estimate is then

$$\widehat{B}_g = \sum_{l=1}^{n_L} \widehat{N}_g(L=l)\widehat{w}(L=l) \tag{5}$$

where $\widehat{w}(L=l)$ is the estimated weight at length from fitting length-weight observations described above. Length is typically measured to the nearest cm so n_L indicates the number of 1 cm length categories that were observed during the survey.

We used length-weight observations for each of the annual NEFSC surveys to estimate length-weight relationships for fall and spring surveys each year and survey catches at length per tow to estimate seasonal and annual biomass estimates with and without diel effects on relative catch efficiency. The methods for these estimates are identical to the descriptions for the first two type of biomass estimates described by in Miller et al. (2017b). For all the models fitted to the twin trawl data, the length-weight data, and the survey data, parameter estimation was performed by maximizing the model likelihood programmed in TMB (Kristensen et al. 2016) and R (R Core Team 2017).

We compared posterior empirical Bayes and bootstrap methods for estimating uncertainty in the relative catch efficiency. We made 1000 bootstrap data sets by randomly drawing with replacement the paired observations from the original twin trawl data. We refit the best performing model to each bootstrap data set and retained the predicted relative efficiency (at size) for each bootstrap. To estimate uncertainty in biomass, we used bootstrap methods for all components of the biomass estimate. Like the relative catch efficiency, bootstrap predictions of weight at length were made by sampling with replacement the length-weight observations within each annual survey and refitting the length-weight relationship to each of the bootstrap datasets. Bootstrap data sets for each of the annual surveys respected the stratified random designs by resampling with replacement within each stratum. For each of the 1000 combined bootstrap results, survey observations for bootstrap b were scaled with the corresponding bootstrap estimates of relative cookie sweep to rockhopper sweep efficiency and predicted weight at length, using Eqs. 4 and 5 for the respective biomass estimation method.

Results

As measured by AIC, the best performing model for the twin-trawl observations included size effects and random variation in relative catch efficiency among observations for all 6 species of flatfish (Table 4). Diel effects on the model parameters was important for 4 species: (summer flounder, windowpane, winter flounder, and witch flounder). Within-haul extra-binomial variation (overdispersion via the beta-binomial assumption) was important for American plaice, yellowtail flounder, and witch flounder. Using the best performing models that assume model parameters are the same for tows made during day and night, the relative efficiency of the chain sweep gear to the rockhopper sweep gear generally declines with increased size (Figure 6). When diel effects on model parameters are assumed the decline is more pronounced when tows are conducted during the day (Figure 7). The increase in efficiency of the chain sweep over the rockhopper sweep is also greater during the day.

Stock-specific trends in annual biomass estimates from 2009 to 2016 for the NEFSC spring and fall survey were generally the same whether $\widehat{B}_1$ or $\widehat{B}_2$ (Eqs. 1 to 5) were used. Spring biomass estimates declined for GB-GOM windowpane, GB yellowtail flounder, and SNE-MA yellowtail flounder, increased for American plaice and GOM winter flounder, and remained relatively stable for other stocks (Tables 5 to 6 and Figures 8 and 11). Fall biomass estiamtes declined for GOM winter founder and GB yellowtail flounder, and SNE-MA yellowtail flounder, increased for American plaice and witch flounder and remained relatively stable for other stocks. However, the uncertainty in the biomass estimates using $\widehat{B}_2$ were generally greater than those using $\widehat{B}_1$ and were particularly problematic for witch flounder, and all three of the yellowtail flounder stocks where bootstrap-based confidence intervals ranged down to zero.

The effective efficiency of the biomass estimates can be inferred by dividing the scaled biomass estimates derived using the relative efficiency of the chain and rockhopper sweeps with the biomass estimates from the unscaled numbers at length observed at each station. Annual values will vary due to the differences in abundance at length. The relative biomass efficiency when using $\widehat{B}_1$ were greatest for American plaice and the winter flounder stocks (approximately 0.7) and the lowest efficiencies were observed for witch flounder and the windowpane stocks (between 0.2 and 0.3) (Figures 12 and 13). The efficiences were similar when $\widehat{B}_2$ are used, but like the biomass estimates themselves, there is greater uncertainty in the ratio estimates with those for witch flounder and the yellowtail stocks ranging up to infinity mirroring the large confidence intervals for the biomass estimates (Figures 14 and 15).

References

Bourne, N. 1965. A comparison of catches by 3- and 4-inch rings on offshore scallop drags .

Gulland, J. A. 1964. Variations in selection factors, and mesh differentials. Journal Du Conseil International Pour L'exploration De La Mer **29**(2): 158–165.

ICES. 1996. Manual of methods of measuring the selectivity of towed fishing gears. (Eds.) Wileman, D. A., Ferro, R. S. T., Fonteyne, R., and Millar, R. B. ICES Cooperative Research Report No. 215.

Kristensen, K., Nielsen, A., Berg, C. W., Skaug, H., and Bell, B. M. 2016. TMB: Automatic differentiation and Laplace approximation. Journal of Statistical Software **70**(5): 1–21.

Miller, T. J. 2013. A comparison of hierarchical models for relative catch efficiency based on paired-gear data for U.S. Northwest Atlantic fish stocks. Canadian Journal of Fisheries and Aquatic Sciences **70**(9): 1306–1316.

Miller, T. J., Martin, M., Politis, P., Legault, C. M., and Blaylock, J. 2017a. Some statistical approaches to combine paired observations of chain sweep and rockhopper gear and catches from NEFSC and DFO trawl surveys in estimating Georges Bank yellowtail flounder biomass. TRAC Working Paper 2017/XX. 36p,.

Miller, T. J., Richardson, D. E., Politis, P., and Blaylock, J. 2017b. NEFSC bottom trawl catch efficiency and biomass estimates for 2009-2017 for 8 flatfish stocks included in the 2017 Northeast Groundfish Operational Assessments. 2017 Groundfish Operational Assessment working paper. Northeast Fisheries Science Center.

Politis, P. J., Galbraith, J. K., Kostovick, P., and Brown, R. W. 2014. Northeast Fisheries Science Center bottom trawl survey protocols for the NOAA Ship Henry B. Bigelow. U.S. Dept. Commer., Northeast Fish. Sci. Cent. Ref. Doc. 14-06, 138p.

R Core Team. 2017. R: A Language and Environment for Statistical Computing. R Foundation for Statistical Computing, Vienna, Austria.

Fig. 1. Diagram of the standard Northeast Fisheries Science Center rockhopper sweep center and wing sections.

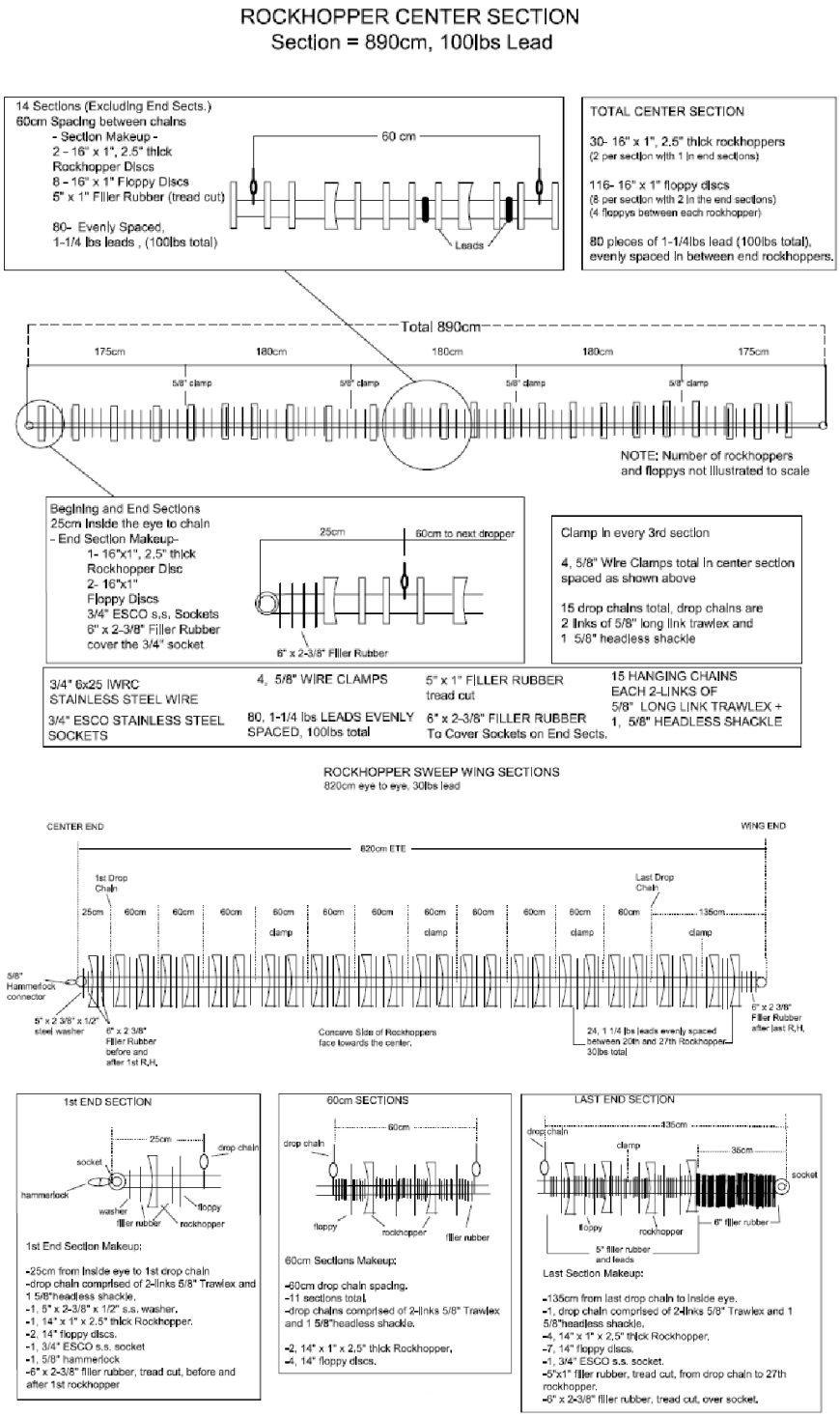

Fig. 2. Diagram of the chain sweep designed maximize bottom contact and flatfish capture.

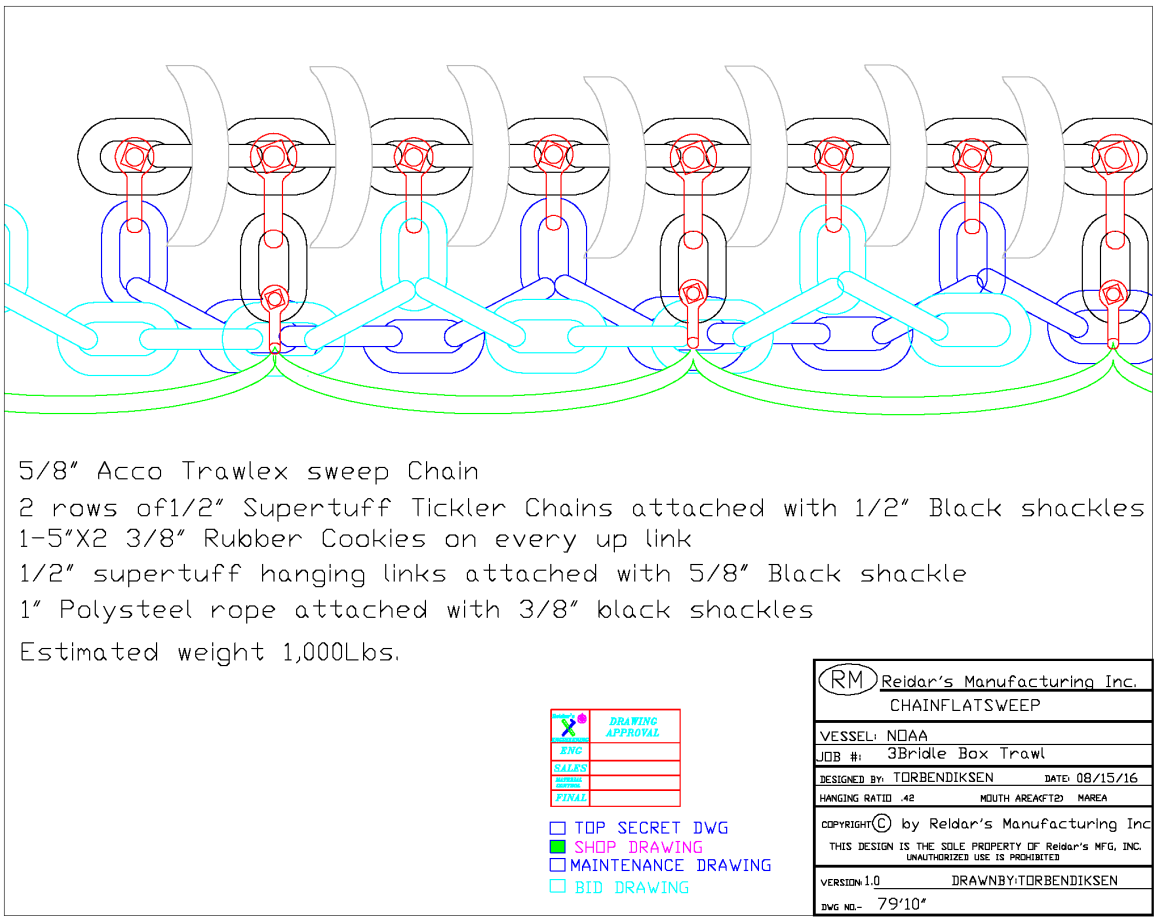

Fig. 3. Locations of stations in 2015 where the F/V Karen Elizabeth conducted twin-trawl sets with the standard bottom trawl gear and the gear with a chain sweep instead of the rockhopper sweep.

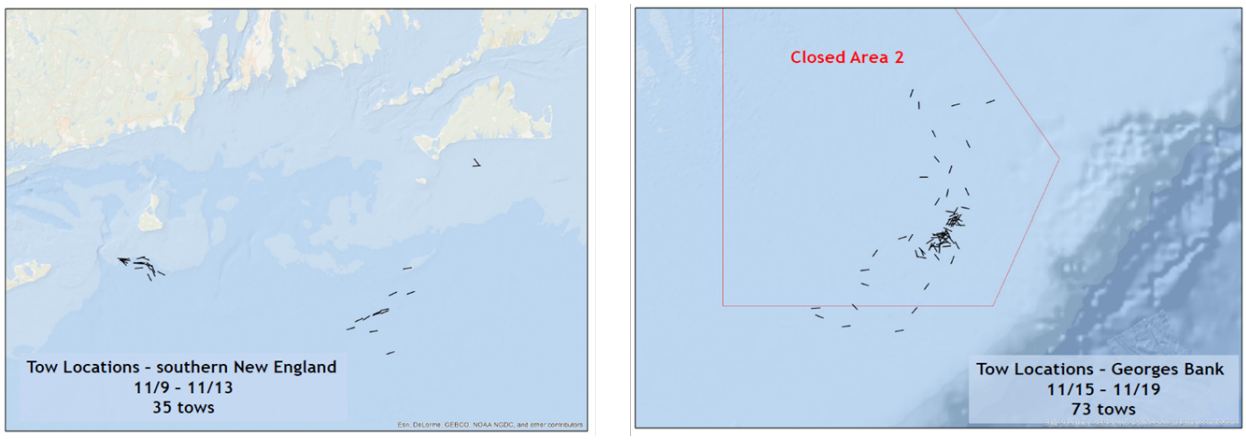

Fig. 4. Locations of stations in 2016 where the F/V Karen Elizabeth conducted twin-trawl sets with the standard bottom trawl gear and the gear with a chain sweep instead of the rockhopper sweep.

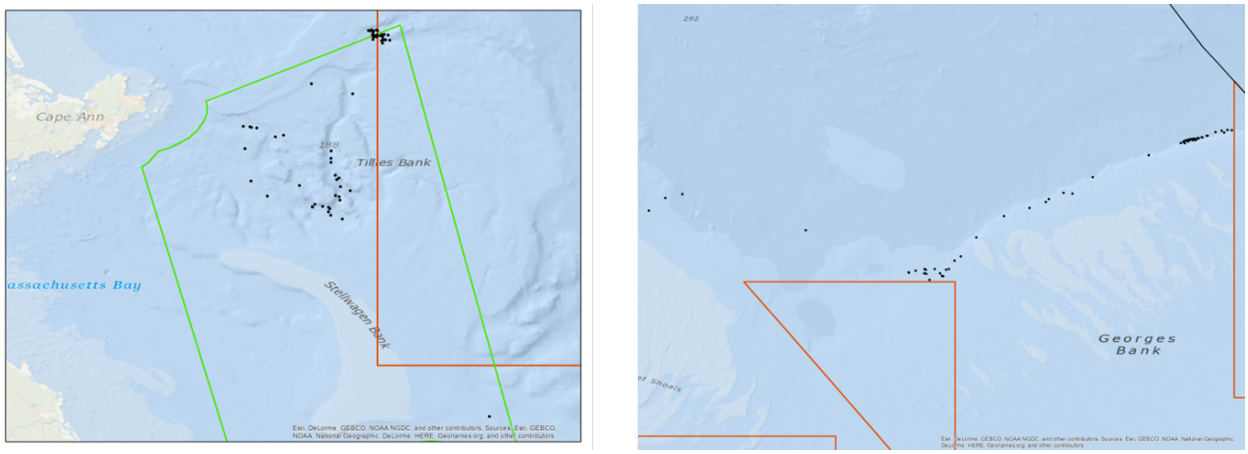

Fig. 5. Locations of stations in 2017 where the F/V Karen Elizabeth conducted twin-trawl sets with the standard bottom trawl gear and the gear with a chain sweep instead of the rockhopper sweep.

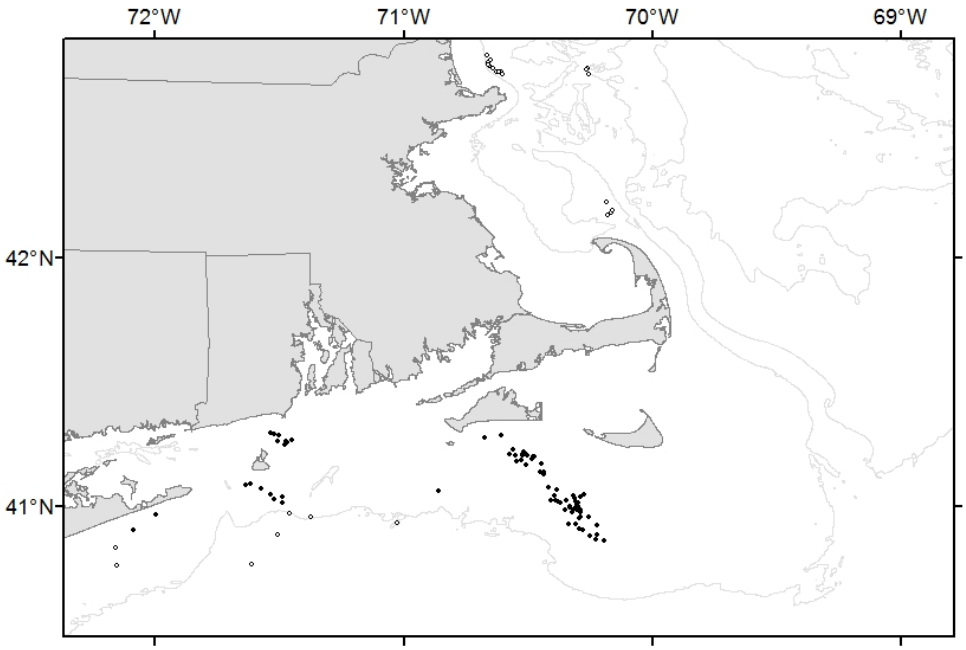

Fig. 6. Estimated relative catch efficiency from best models with all parameters the same for tows during day and night. Black and grey lines are for mean and tow-specific relative catch efficiencies, respectively. Gray polygons and dashed red lines reflect 95% confidence intervals using derived from delta method-based variance estimates and bootstrap quantiles, respectively.

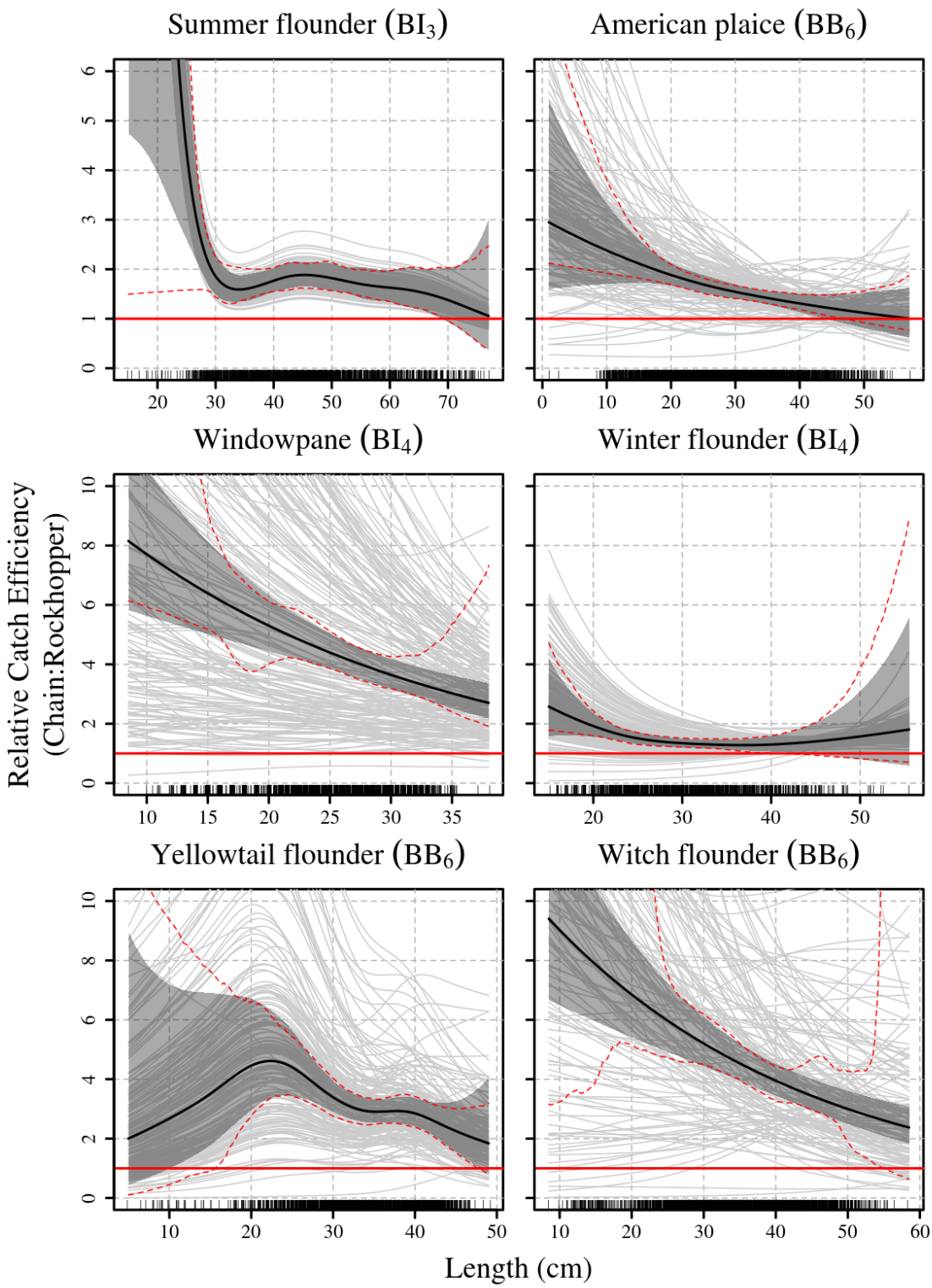

Fig. 7. Estimated relative catch efficiency from best models with all parameters differing for tows during the day and night. Black and grey lines are for mean and tow-specific relative catch efficiencies, respectively. Gray polygons and dashed red lines reflect 95% confidence intervals derived from delta method-based variance estimates and bootstrap quantiles, respectively.

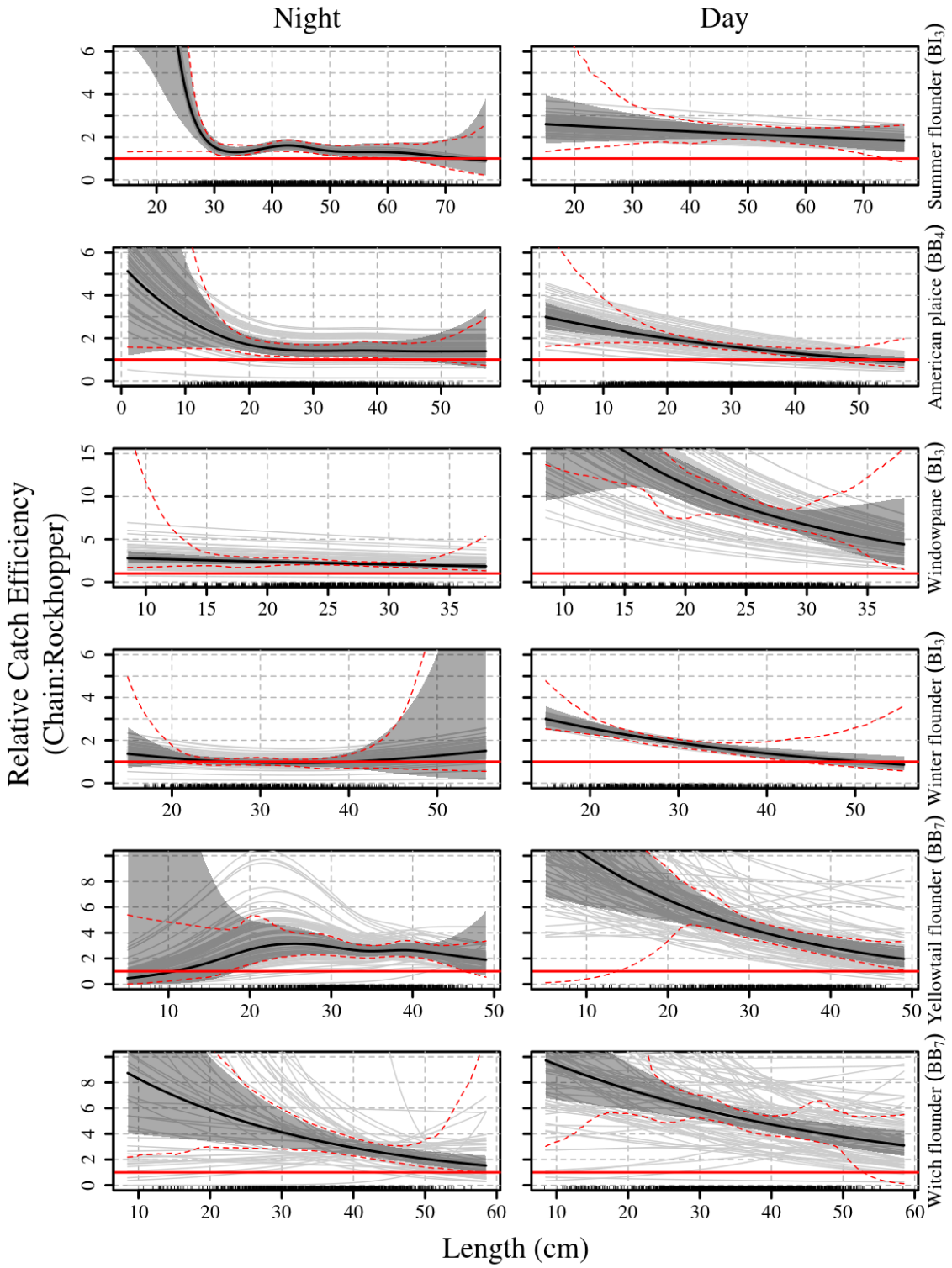

Fig. 8. Estimated annual chain sweep-based biomass for summer flounder, American plaice, witch flounder, and GB-GOM and SNE-MAB windowpane during the fall and spring surveys between 2009 and 2016. Estimates use relative catch efficiency from best models with all parameters the same for tows during the day and night. Gray polygons reflect 95% confidence intervals derived from bootstrap quantiles.

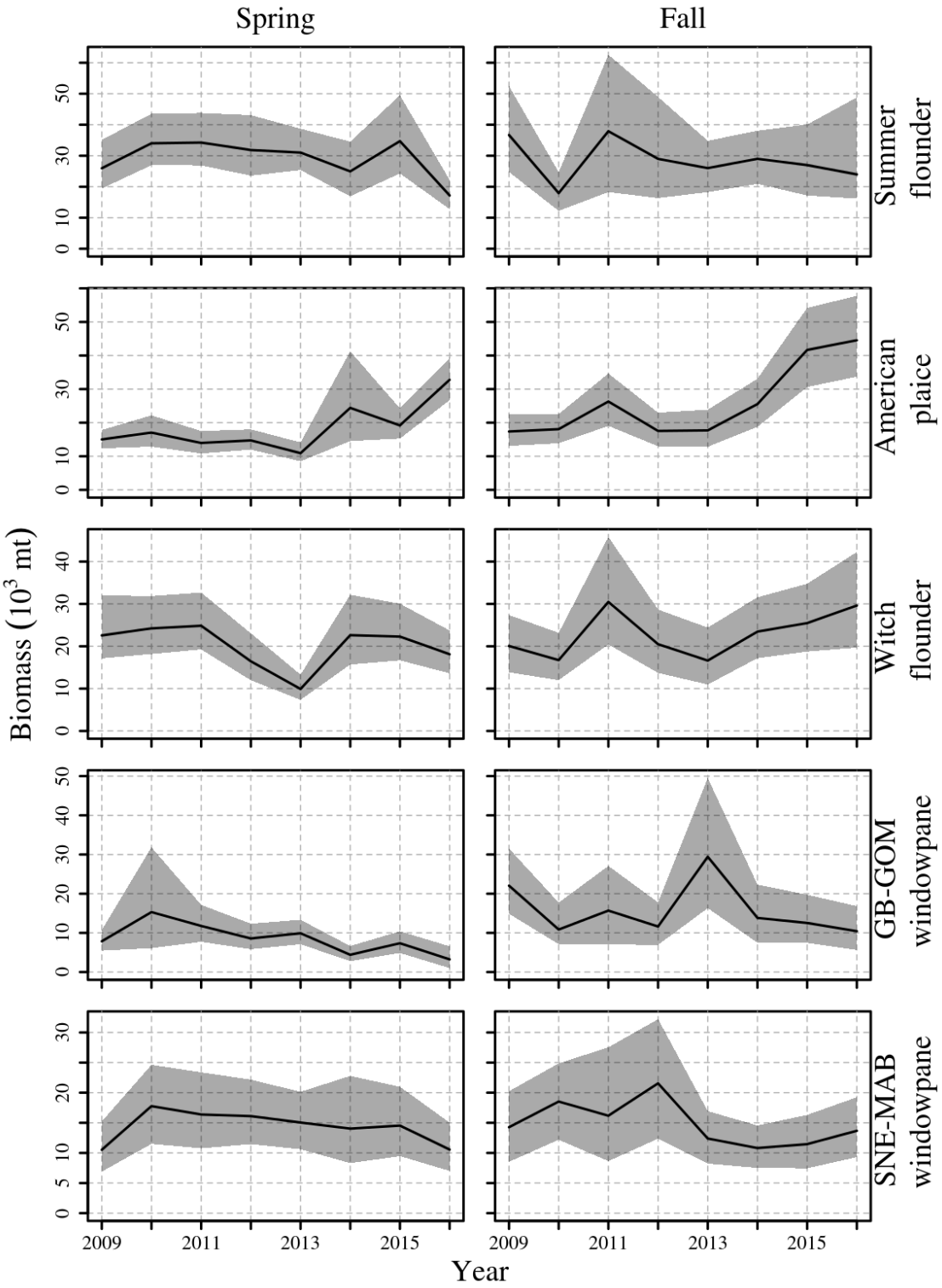

Fig. 9. Estimated annual chain sweep-based biomass for GB, GOM and SNE winter flounder, and GB, SNE-MA, and CC-GOM yellowtail flounder during the fall and spring surveys between 2009 and 2016. Estimates use relative catch efficiency from best models with all parameters the same for tows during the day and night. Gray polygons reflect 95% confidence intervals derived from bootstrap quantiles.

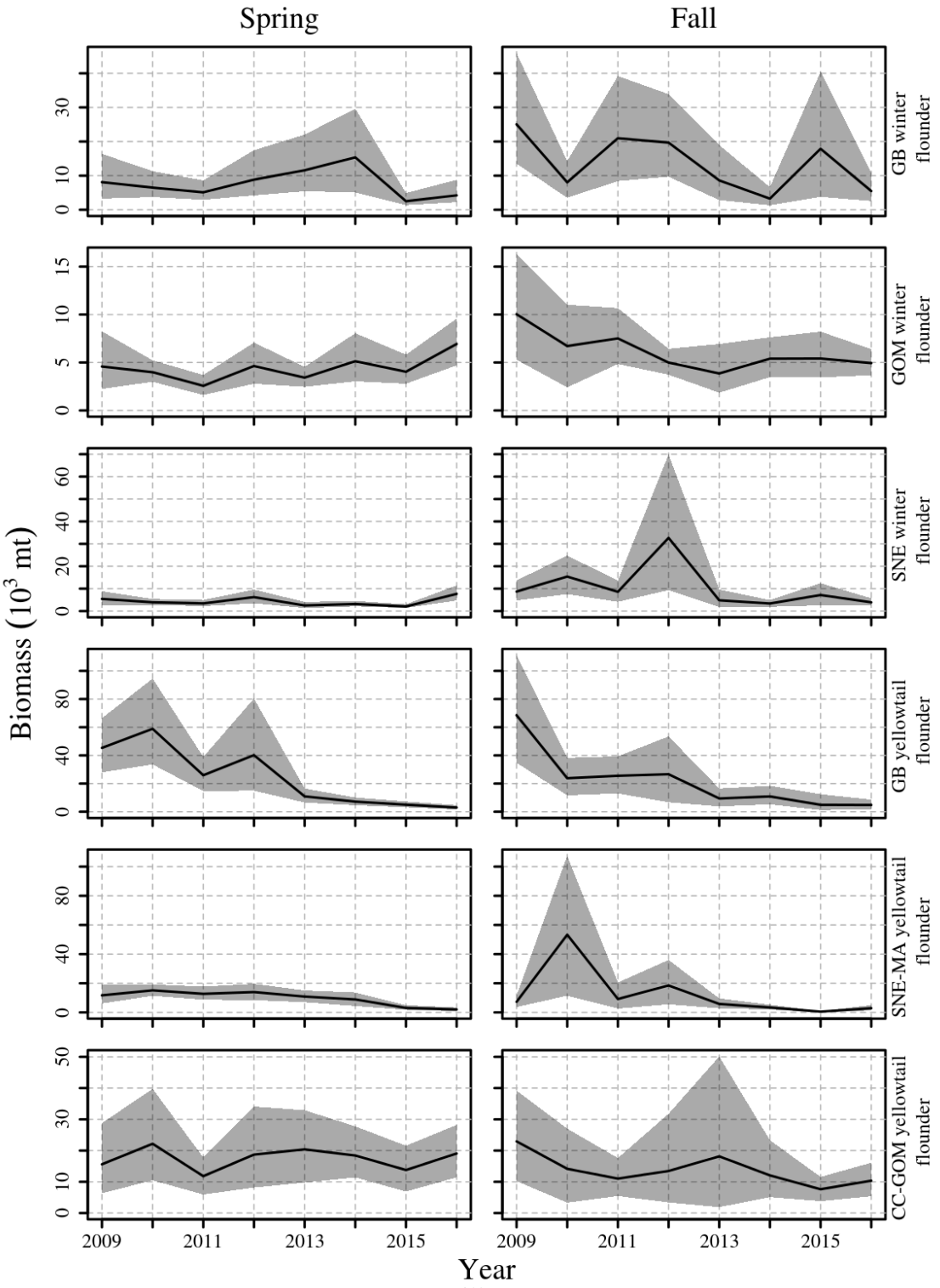

Fig. 10. Estimated annual chain sweep-based biomass for summer flounder, American plaice, witch flounder, and GB-GOM and SNE-MAB windowpane during the fall and spring surveys between 2009 and 2016. Estimates use relative catch efficiency from best models with all parameters differing for tows during the day and night. Gray polygons reflect 95% confidence intervals derived from bootstrap quantiles.

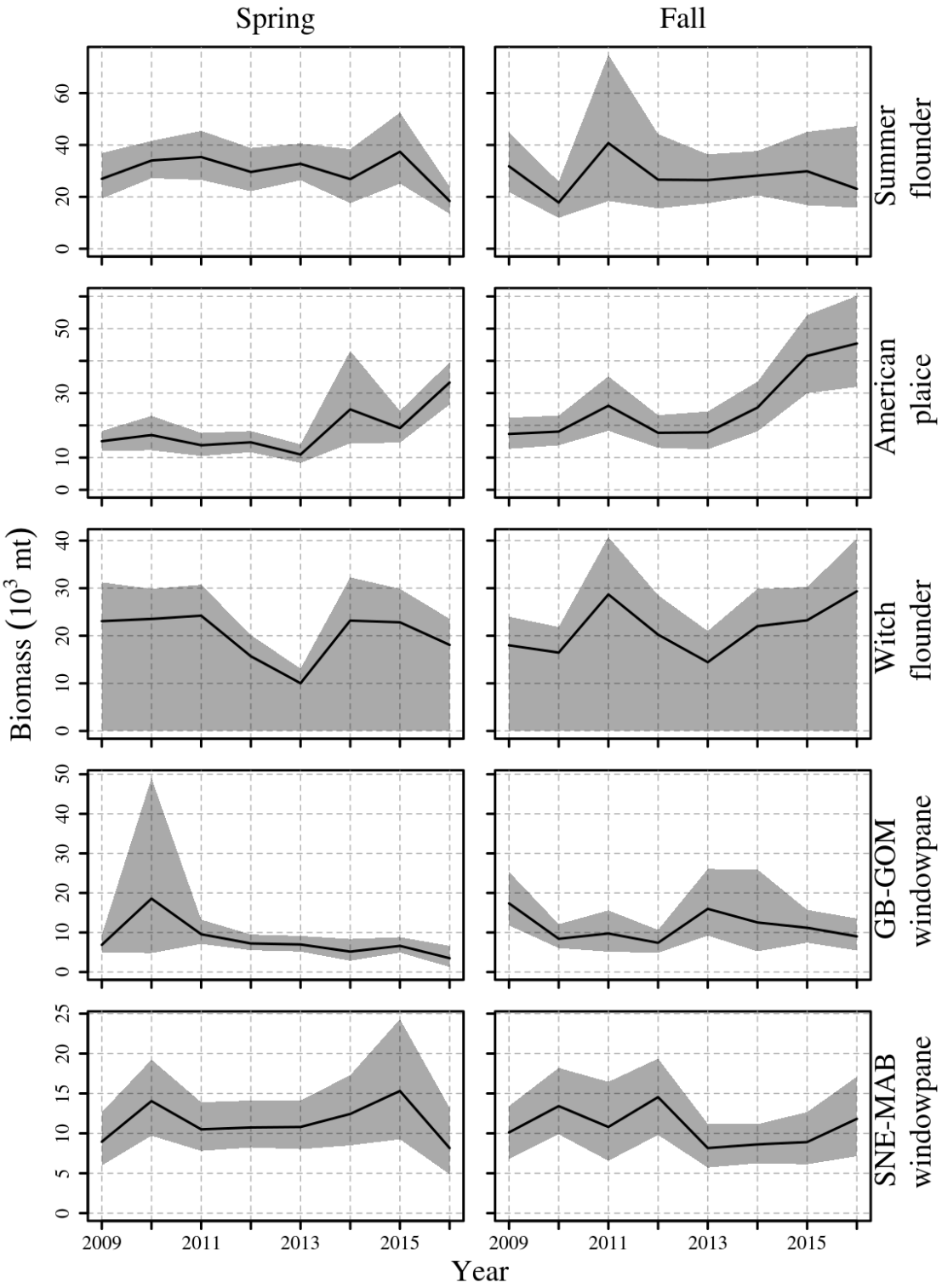

Fig. 11. Estimated annual chain sweep-based biomass for GB, GOM and SNE winter flounder, and GB, SNE-MA, and CC-GOM yellowtail flounder during the fall and spring surveys between 2009 and 2016. Estimates use relative catch efficiency from best models with all parameters differing for tows during the day and night. Gray polygons reflect 95% confidence intervals derived from bootstrap quantiles.

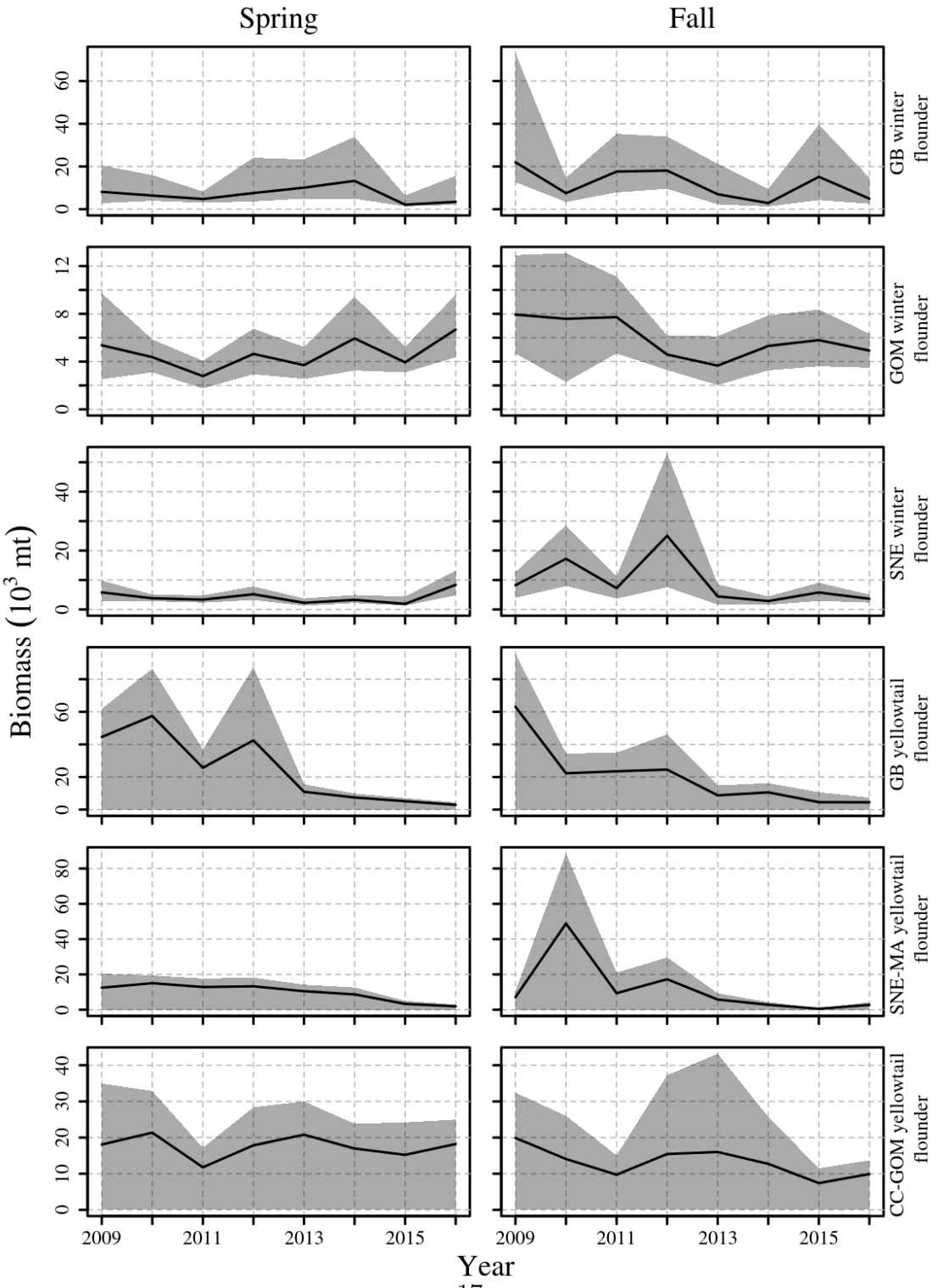

Fig. 12. Estimated effective efficiency of rock-hopper sweep for biomass of summer flounder, American plaice, witch flounder, and GB-GOM and SNE-MAB windowpane during the fall and spring surveys between 2009 and 2016. Estimates divide the biomass estimates from unscaled catches from the survey by the biomass estimates from scaling observed catches using relative catch efficiency at size from best models with all parameters the same for tows during the day and night. Gray polygons reflect 95% confidence intervals derived from bootstrap quantiles.

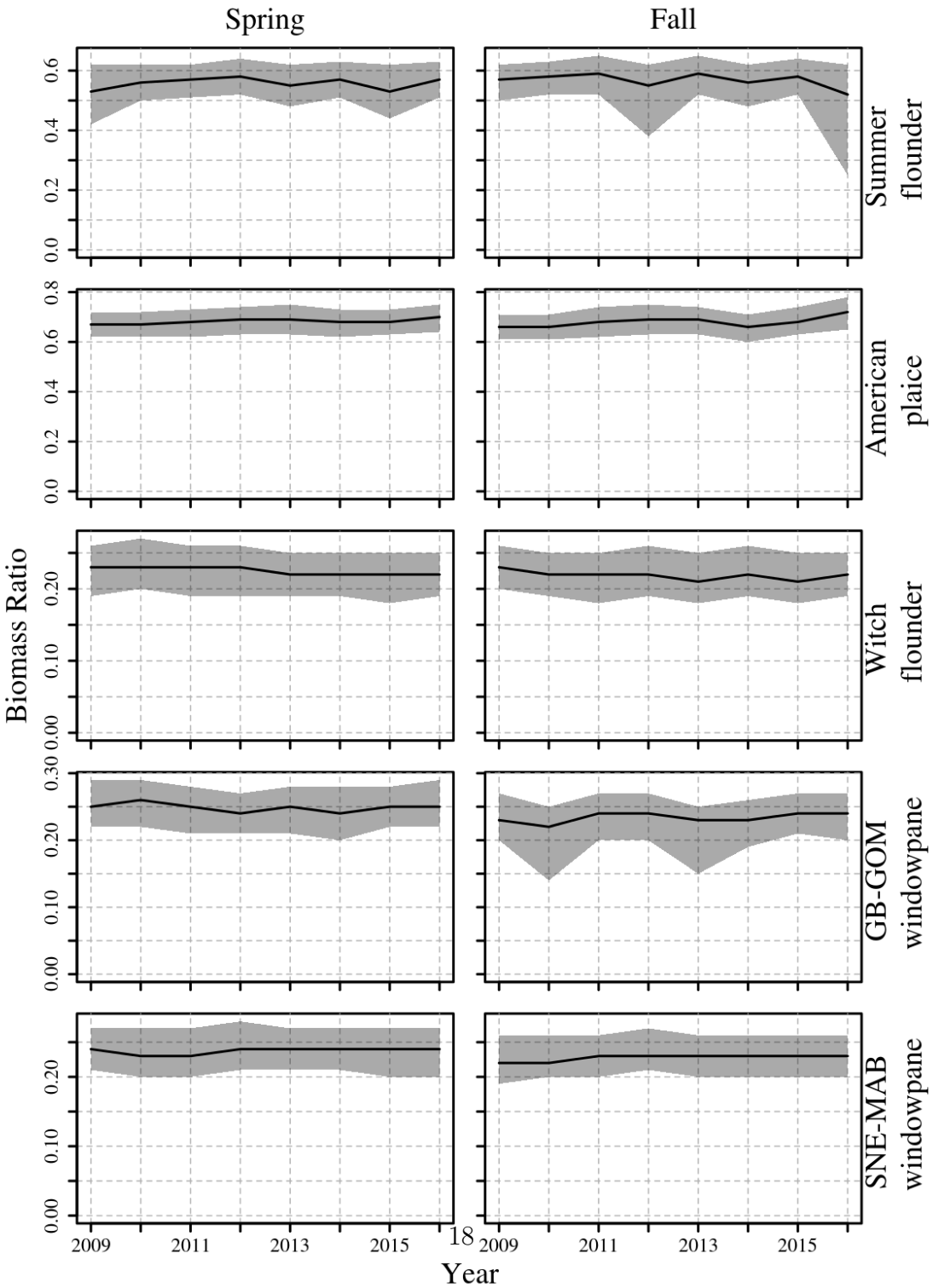

Fig. 13. Estimated effective efficiency of rock-hopper sweep for biomass of GB, GOM and SNE winter flounder, and GB, SNE-MA, and CC-GOM yellowtail flounder during the fall and spring surveys between 2009 and 2016. Estimates divide the biomass estimates from unscaled catches from the survey by the biomass estimates from scaling observed catches using relative catch efficiency at size from best models with all parameters the same for tows during the day and night. Gray polygons reflect 95% confidence intervals derived from bootstrap quantiles.

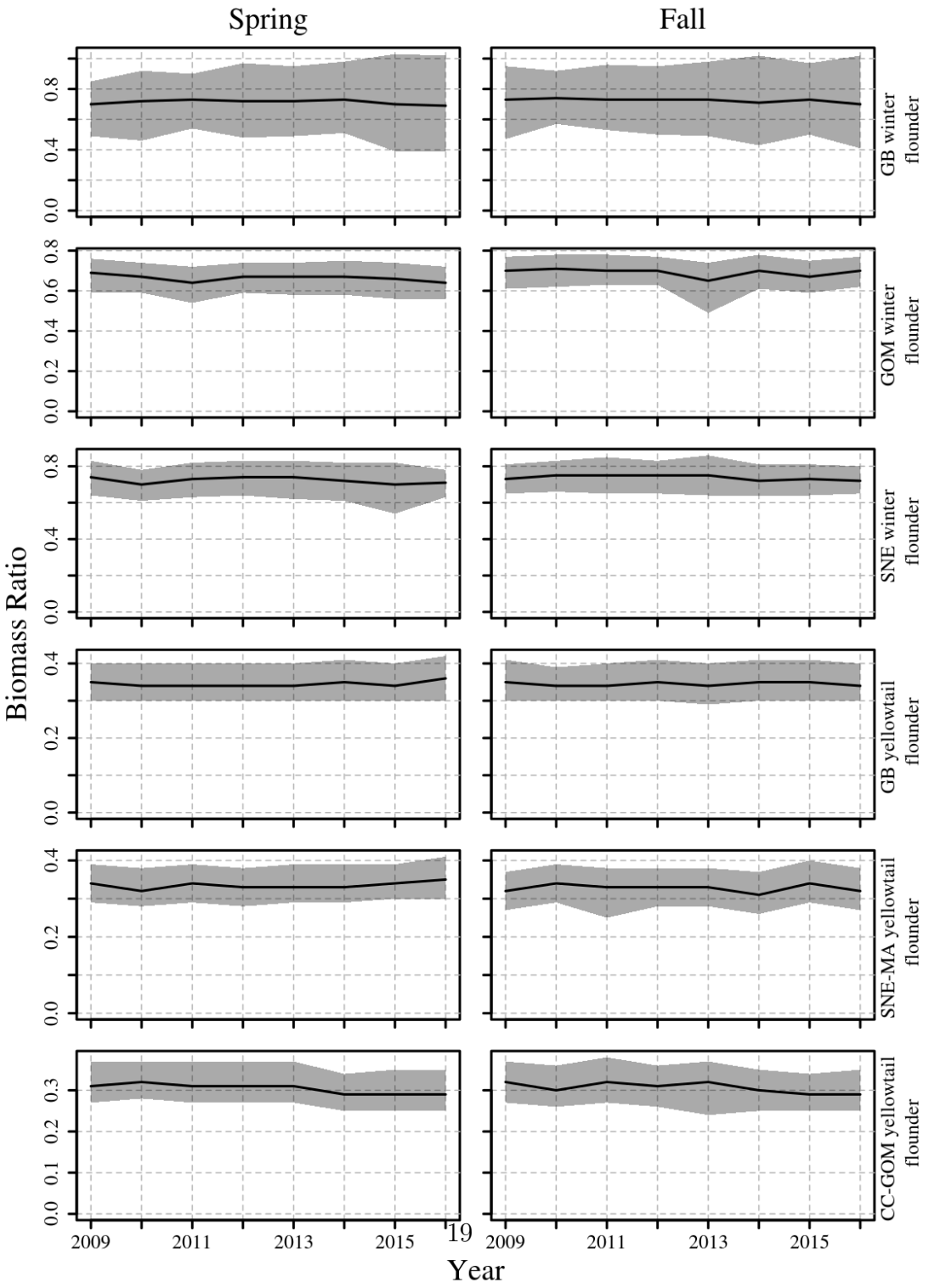

Fig. 14. Estimated effective efficiency of rock-hopper sweep for biomass of summer flounder, American plaice, witch flounder, and GB-GOM and SNE-MAB windowpane during the fall and spring surveys between 2009 and 2016. Estimates divide the biomass estimates from unscaled catches from the survey by the biomass estimates from scaling observed catches using relative catch efficiency at size from best models with all parameters differing for tows during the day and night. Gray polygons reflect 95% confidence intervals derived from bootstrap quantiles.

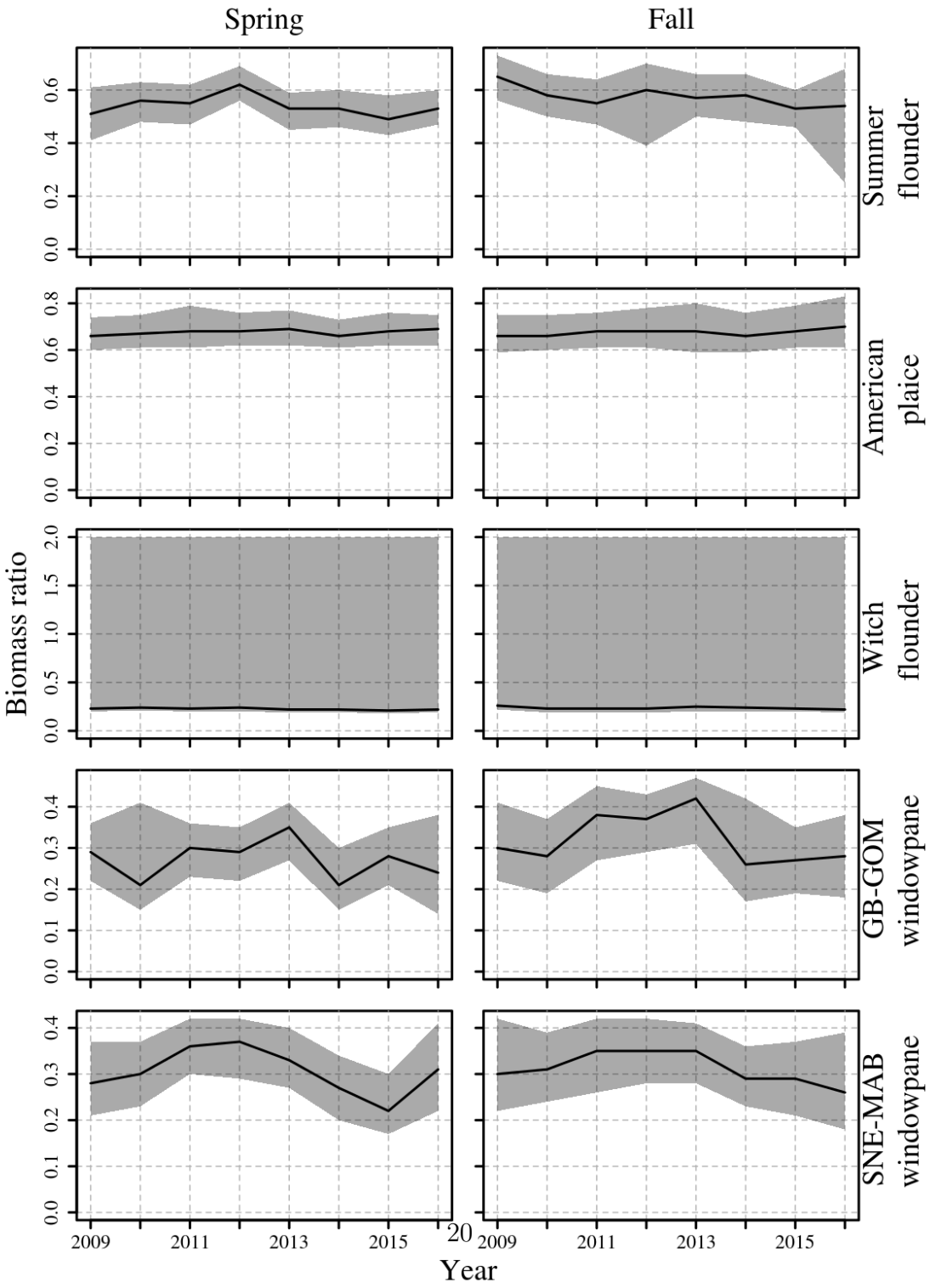

Fig. 15. Estimated effective efficiency of rock-hopper sweep for biomass of GB, GOM and SNE winter flounder, and GB, SNE-MA, and CC-GOM yellowtail flounder during the fall and spring surveys between 2009 and 2016. Estimates divide the biomass estimates from unscaled catches from the survey by the biomass estimates from scaling observed catches using relative catch efficiency at size from best models with all parameters differing for tows during the day and night. Gray polygons reflect 95% confidence intervals derived from bootstrap quantiles.

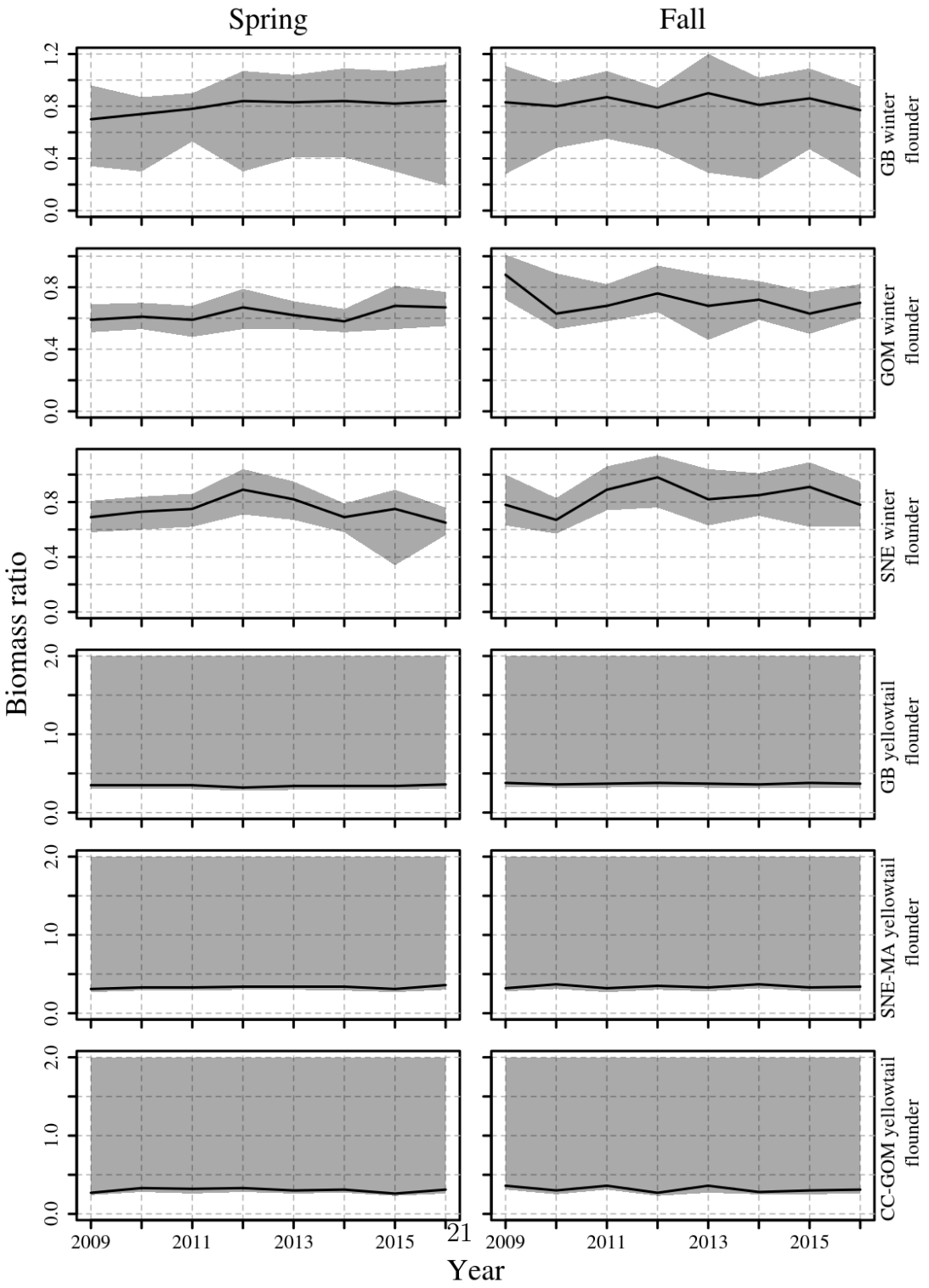

Table 1. Number of twin-trawl tows conducted where each species was caught during the day, night, and in total.

Species	Day	Night	Total
Summer flounder	73	66	139
American plaice	84	51	135
Windowpane	93	93	186
Winter flounder	94	73	167
Yellowtail flounder	86	81	167
Witch flounder	83	49	132

Table 2. Description of relative catch efficiency (ρ) parameterizations for conditional binomial models fit to data for each species.

Model	$\log(\rho)$	Across-pair effects	Pair-specific random effects
BI_0	β_0	intercept	none
BI_1	$\beta_0 + \delta_{0,j}$	intercept	intercept
BI_2	$\mathbf{X}_f^T\boldsymbol{\beta} + \mathbf{X}_r^T\mathbf{b}$	intercept and cubic spline smoother of size	none
BI_3	$\mathbf{X}_f^T\boldsymbol{\beta} + \mathbf{X}_r^T\mathbf{b} + \delta_{0,j}$	intercept and cubic spline smoother of size	intercept
BI_4	$\mathbf{X}_f^T(\boldsymbol{\beta}_f + \boldsymbol{\delta}_j) + \mathbf{X}_r^T(\mathbf{b} + \boldsymbol{\epsilon}_j)$	intercept and cubic spline smoother of size	intercept and cubic spline smoother of size

Table 3. Description of relative catch efficiency (ρ) and dispersion (ϕ) parameterizations for conditional beta-binomial models fit to data for each species.

Model	$\log(\rho)$	$\log(\phi)$	Across-pair effects	Pair-specific random effects
BB_0	β_0	γ_0	intercepts for mean and dispersion	none
BB_1	$\beta_0 + \delta_{0,j}$	γ_0	intercepts for mean and dispersion	intercept for mean
BB_2	$\mathbf{X}_f^T\boldsymbol{\beta} + \mathbf{X}_r^T\mathbf{b}$	γ_0	mean and dispersion intercepts and cubic-spline smoother of size for mean	none
BB_3	$\mathbf{X}_f^T\boldsymbol{\beta} + \mathbf{X}_r^T\mathbf{b}$	$\mathbf{X}_f^T\boldsymbol{\gamma} + \mathbf{X}_r^T\mathbf{g}$	intercepts and cubic-spline smoothers of size for mean and dispersion	none
BB_4	$\mathbf{X}_f^T\boldsymbol{\beta} + \mathbf{X}_r^T\mathbf{b} + \delta_{0,j}$	γ_0	mean and dispersion intercepts and cubic-spline smoother of size for mean	intercept for mean
BB_5	$\mathbf{X}_f^T\boldsymbol{\beta} + \mathbf{X}_r^T\mathbf{b} + \delta_{0,j}$	$\mathbf{X}_f^T\boldsymbol{\gamma} + \mathbf{X}_r^T\mathbf{g}$	intercepts and cubic-spline smoothers of size for mean and dispersion	intercept for mean
BB_6	$\mathbf{X}_f^T(\boldsymbol{\beta}_f + \boldsymbol{\delta}_j) + \mathbf{X}_r^T(\mathbf{b} + \boldsymbol{\epsilon}_j)$	γ_0	mean and dispersion intercepts and cubic-spline smoother of size for mean	intercept and cubic spline smoother for mean
BB_7	$\mathbf{X}_f^T(\boldsymbol{\beta}_f + \boldsymbol{\delta}_j) + \mathbf{X}_r^T(\mathbf{b} + \boldsymbol{\epsilon}_j)$	$\mathbf{X}_f^T\boldsymbol{\gamma} + \mathbf{X}_r^T\mathbf{g}$	intercepts and cubic-spline smoothers of size for mean and dispersion	intercept and cubic spline smoother for mean

Table 4. Difference in AIC between specific model and that with the lowest AIC (ΔAIC) for each species. Combined models assume no model parameters differ for tows conducted during day and night whereas day/night-specific models assume all parameters differ for tows conducted during day and night.

Model		**ΔAIC**					
	n_p	Summer flounder	American plaice	Windowpane	Winter flounder	Yellowtail flounder	Witch flounder
Combined							
BI_0	1	46.40	876.59	1183.24	273.86	717.32	1628.61
BI_1	2	32.55	544.49	178.06	73.39	89.41	253.18
BI_2	3	27.24	799.27	1167.35	257.73	719.24	1567.98
BI_3	4	19.03	493.67	156.26	60.64	51.32	178.41
BI_4	7		417.08	139.00	57.57	11.09	72.39
BB_0	2	47.12	223.55	723.97	220.63	385.95	1047.05
BB_1	3	34.47	68.88	171.73	74.29	61.79	182.62
BB_2	4	28.96	185.41	710.55	208.98	384.88	1003.42
BB_3	6			707.68	208.35	365.25	
BB_4	5		34.45	154.49	61.83	31.23	119.85
BB_5	7			152.09	64.39	29.63	
BB_6	8		0.00	140.93	58.97	0.00	36.80
BB_7	10			145.19		3.36	
Day/Night-specific							
BI_0	2	23.18	864.50	253.18	78.44	520.41	1373.13
BI_1	4	16.51	535.62	27.54	14.31	81.04	236.34
BI_2	6	1.57	791.10	228.50	62.44	455.58	1297.39
BI_3	8	0.00	481.14	0.00	0.00	28.67	161.85
BI_4	14						54.12
BB_0	4	26.50	207.30	173.18	65.37	295.52	924.29
BB_1	6		52.37	22.54	17.33	55.05	167.43
BB_2	8	5.51	169.19	160.84	50.49	266.96	869.82
BB_3	12			164.85	54.59	238.84	849.38
BB_4	10		16.49	2.35	3.23	9.62	104.61
BB_5	14		18.36		10.22	16.07	73.86
BB_6	16						19.92
BB_7	20					5.41	0.00

Table 5. Estimated chain sweep swept area spring survey biomass (mt) for each stock between 2009 and 2016 using relative efficiency estimates from models with parameters that do not differ for tows conducted during day and night.

Year	Fluke	American plaice	GB-GOM windowpane	SNE-MAB windowpane	GB winter flounder	GOM winter flounder	SNE winter flounder	GB yellowtail flounder	SNE-MA yellowtail flounder	CC-GOM yellowtail flounder	Witch flounder
2009	25,954	15,013	7,851	10,516	8,103	4,578	5,428	45,327	11,708	15,614	22,565
2010	34,024	17,051	15,302	17,771	6,497	3,987	3,927	58,853	15,142	22,181	24,227
2011	34,248	13,965	11,767	16,383	5,115	2,565	3,422	25,909	12,741	11,805	24,854
2012	31,838	14,726	8,570	16,112	8,828	4,631	6,232	40,167	13,974	18,710	16,445
2013	31,025	10,921	9,905	15,046	11,571	3,418	2,515	10,910	10,868	20,383	9,913
2014	24,955	24,409	4,406	14,039	15,359	5,132	3,160	7,169	8,890	18,416	22,626
2015	34,713	19,192	7,357	14,543	2,507	4,034	2,060	5,022	3,059	13,768	22,289
2016	17,186	32,774	3,246	10,558	4,230	6,930	7,679	3,004	1,997	19,068	18,117

Table 6. Estimated chain sweep swept area fall survey biomass (mt) for each stock between 2009 and 2016 using relative efficiency estimates from models with parameters that do not differ for tows conducted during day and night.

Year	Fluke	American plaice	GB-GOM windowpane	SNE-MAB windowpane	GB winter flounder	GOM winter flounder	SNE winter flounder	GB yellowtail flounder	SNE-MA yellowtail flounder	CC-GOM yellowtail flounder	Witch flounder
2009	36,689	17,378	22,049	14,274	25,051	10,034	8,724	68,523	7,242	22,944	20,069
2010	17,927	18,076	10,858	18,526	8,042	6,713	15,372	23,814	53,291	14,156	16,730
2011	37,913	26,310	15,683	16,180	20,978	7,506	8,621	25,563	9,177	11,024	30,483
2012	28,991	17,541	11,632	21,556	19,688	4,992	32,668	26,648	18,470	13,462	20,490
2013	26,004	17,709	29,424	12,393	8,611	3,851	4,815	9,416	5,808	18,140	16,617
2014	29,004	25,540	13,823	10,816	3,260	5,399	3,381	10,858	3,366	12,057	23,455
2015	26,977	41,659	12,531	11,461	17,880	5,414	7,175	4,926	527	7,619	25,472
2016	23,978	44,549	10,431	13,673	5,488	4,935	3,910	4,816	2,891	10,364	29,620

Table 7. Estimated chain sweep swept area spring survey biomass (mt) for each stock between 2009 and 2016 using relative efficiency estimates from models with parameters that differ for tows conducted during day and night.

Year	Fluke	American plaice	GB-GOM windowpane	SNE-MAB windowpane	GB winter flounder	GOM winter flounder	SNE winter flounder	GB yellowtail flounder	SNE-MA yellowtail flounder	CC-GOM yellowtail flounder	Witch flounder
2009	26,941	15,100	6,883	8,947	8,150	5,366	5,798	44,526	12,508	18,061	23,072
2010	34,014	16,991	18,562	14,045	6,385	4,373	3,807	57,438	15,053	21,359	23,536
2011	35,354	13,852	9,564	10,505	4,783	2,778	3,331	25,662	12,890	11,774	24,224
2012	29,614	14,750	7,229	10,737	7,576	4,644	5,174	42,476	13,278	17,845	15,691
2013	32,742	10,960	6,976	10,800	10,083	3,705	2,269	10,947	10,519	20,790	10,026
2014	26,834	24,949	5,159	12,429	13,260	5,941	3,277	7,426	8,694	16,965	23,194
2015	37,399	19,145	6,621	15,315	2,132	3,939	1,907	5,144	3,307	15,212	22,833
2016	18,411	33,287	3,508	8,154	3,462	6,689	8,368	2,932	1,918	18,223	18,084

Table 8. Estimated chain sweep swept area fall survey biomass (mt) for each stock between 2009 and 2016 using relative efficiency estimates from models with parameters that differ for tows conducted during day and night.

Year	Fluke	American plaice	GB-GOM windowpane	SNE-MAB windowpane	GB winter flounder	GOM winter flounder	SNE winter flounder	GB yellowtail flounder	SNE-MA yellowtail flounder	CC-GOM yellowtail flounder	Witch flounder
2009	31,790	17,339	17,365	10,118	21,976	7,938	8,208	63,077	7,095	19,894	17,995
2010	17,816	18,076	8,415	13,415	7,493	7,584	17,220	22,285	48,858	14,061	16,461
2011	40,734	26,095	9,759	10,798	17,623	7,725	7,235	23,499	9,391	9,724	28,687
2012	26,638	17,693	7,394	14,541	18,085	4,588	25,017	24,547	17,278	15,454	20,233
2013	26,481	17,832	15,967	8,161	6,997	3,661	4,449	8,746	5,771	16,010	14,448
2014	28,162	25,511	12,542	8,616	2,859	5,308	2,861	10,589	2,815	12,723	22,004
2015	29,872	41,528	11,198	8,910	15,141	5,799	5,777	4,562	541	7,401	23,247
2016	23,082	45,400	9,025	11,816	4,954	4,925	3,632	4,500	2,741	9,896	29,340